

Biochemical and structural characterization of the GTP-preferring succinyl-CoA synthetase from *Thermus aquaticus*

Michael A. Joyce,^{a,‡} Koto Hayakawa,^b William T. Wolodko^a and Marie E. Fraser^{b*}

^aDepartment of Biochemistry, University of Alberta, Edmonton, Alberta T6G 2H7, Canada, and ^bDepartment of Biological Sciences, University of Calgary, 2500 University Drive NW, Calgary, Alberta T2N 1N4, Canada

‡ Current address: Department of Medical Microbiology and Immunology, University of Alberta, Edmonton, Alberta T6G 2H7, Canada.

Correspondence e-mail: frasm@ucalgary.ca

Succinyl-CoA synthetase (SCS) from *Thermus aquaticus* was characterized biochemically *via* measurements of the activity of the enzyme and determination of its quaternary structure as well as its stability and refolding properties. The enzyme is most active between pH 8.0 and 8.4 and its activity increases with temperature to about 339 K. Gel-filtration chromatography and sedimentation equilibrium under native conditions demonstrated that the enzyme is a heterotetramer of two α -subunits and two β -subunits. The activity assays showed that the enzyme uses either ADP/ATP or GDP/GTP, but prefers GDP/GTP. This contrasts with *Escherichia coli* SCS, which uses GDP/GTP but prefers ADP/ATP. To understand the nucleotide preference, *T. aquaticus* SCS was crystallized in the presence of GDP, leading to the determination of the structure in complex with GDP-Mn²⁺. A water molecule and Pro20 β in *T. aquaticus* take the place of Gln20 β in pig GTP-specific SCS, interacting well with the guanine base and other residues of the nucleotide-binding site. This leads to the preference for GDP/GTP, but does not hinder the binding of ADP/ATP.

Received 4 January 2012

Accepted 12 March 2012

PDB Reference: succinyl-CoA synthetase, 3ufx.

1. Introduction

In the citric acid cycle, succinyl-CoA synthetase (SCS) catalyzes the reaction succinyl-CoA + NDP + P_i \rightleftharpoons succinate + CoA + NTP, where N denotes adenosine or guanosine. The reaction requires divalent cations, usually Mg²⁺. The majority of the research investigating SCS has used enzymes from two sources: *Escherichia coli* and pig heart (reviewed by Bridger, 1974; Nishimura, 1986). *E. coli* SCS can use either ADP/ATP or GDP/GTP, but the adenine base is preferred. The enzyme that has been purified from pig heart is GTP-specific, but pigs are one of the many organisms that have two SCS isozymes, each specific for a single nucleotide. SCSs from different species exhibit either a heterodimeric quaternary structure consisting of one α -subunit and one β -subunit, as observed in pig GTP-specific SCS (Brownie & Bridger, 1972), or a heterotetrameric quaternary structure (Bridger, 1971) consisting of a dimer of $\alpha\beta$ dimers, as observed in *E. coli* SCS (Wolodko *et al.*, 1986, 1994). The nucleotide specificity is determined by the β -subunit, since the two isozymes contain a common α -subunit but different β -subunits (Johnson, Muhonen *et al.*, 1998; Johnson, Mehus *et al.*, 1998). The structures of both *E. coli* and pig GTP-specific SCS have been determined using X-ray crystallography (Wolodko *et al.*, 1994; Fraser *et al.*, 1999, 2000, 2006; Joyce *et al.*, 2000).

Very little is known about the properties of SCS from thermophiles. SCS from *Thermus aquaticus* has been shown to exist in the 'large form' with a relative molecular weight of around 150 000, like *E. coli* SCS (Weitzman & Kinghorn, 1983). It was shown to be more thermostable than *E. coli* SCS in a test that consisted of heating the enzyme for 5 min at each temperature, cooling the solution and assaying the activity at a lower temperature. A thermophilic form of SCS could be a useful reagent in experiments using SCS in a coupled enzyme assay to determine the concentration of succinate in solution (Luo *et al.*, 2006), since the thermostability of the enzyme could lead to a simplified purification scheme. With the goal of obtaining pure thermophilic enzyme, SCS from *T. aquaticus* was cloned and overexpressed in *E. coli* and the purified enzyme was crystallized (Joyce *et al.*, 2007). Here, we present the biochemical characterization of *T. aquaticus* SCS via measurements of the activity and quaternary structure of the enzyme as well as its stability and refolding properties. The activity assays showed that *T. aquaticus* SCS uses either ADP/ATP or GDP/GTP but prefers GDP/GTP. This led to crystallization of the enzyme with GDP and determination of the structure in complex with GDP-Mn²⁺. The residues that lead to the preference for GDP are outlined on the basis of comparisons with the structures of *E. coli* SCS in complex with ADP-Mg²⁺ (Joyce *et al.*, 2000) and pig GTP-specific SCS in complex with GTP-K⁺ or GDP-K⁺ (Fraser *et al.*, 2006).

2. Materials and methods

T. aquaticus SCS was purified as described previously (Joyce *et al.*, 2007) and stored either as an ammonium sulfate suspension (20 g ammonium sulfate per 100 ml initial solution) or at 193 K in 20 µl aliquots quick-frozen in liquid nitrogen (Deng *et al.*, 2004). For all experiments except the crystallization, the ammonium sulfate suspension was collected by centrifugation at 15 000g and 277 K for 30 min and the pellet was dissolved in a minimal volume of 50 mM KCl, 0.1 mM EDTA, 50 mM Tris HCl pH 7.4. The resultant solution was clarified by centrifugation and dialyzed for 16 h with three changes of the same buffer, all at 277 K. For the crystallization experiments, the enzyme solution stored at 193 K was thawed and used directly.

2.1. Enzymatic activity

The ability of *T. aquaticus* SCS to catalyze the formation of succinyl-CoA from ATP, CoA and succinate was tested over the pH range 6.2–9.6. A 1.9 µg sample of enzyme was diluted in 1 ml buffer consisting of 10 mM MgCl₂, 50 mM KCl, 0.1 mM dithiothreitol (DTT), 10 mM succinate, 0.1 mM CoA, 0.4 mM ATP and either 50 mM MOPS (pH 6.2–8.2) or 50 mM Tris-HCl (pH 8.0–9.6) and the formation of the thioester bond in succinyl-CoA was measured spectrophotometrically at 235 nm.

For kinetic analyses, enzymatic activity was measured spectrophotometrically in the direction of succinyl-CoA formation at 295 K. The initial velocity was measured in duplicate at various concentrations of one substrate and constant, saturating concentrations of the other substrates.

The concentration ranges for the substrates were 2.50–60.0 µM CoA, 0.125–6.00 mM succinate, 12.5–400 µM ATP and 2.00–100 µM GTP, and the constant concentrations were 114 µM CoA, 10.0 mM succinate or 405 µM ATP or GTP, where appropriate, in a total volume of 1 ml containing 10 mM MgCl₂, 50 mM KCl, 50 mM Tris-HCl pH 8.0. The concentrations of the nucleotides and CoA were determined using their standard extinction coefficients for a 1 cm path length: ATP, $\epsilon_{259\text{ nm}} = 15.4\text{ mM}^{-1}$; GTP, $\epsilon_{252\text{ nm}} = 13.7\text{ mM}^{-1}$; CoA, $\epsilon_{260\text{ nm}} = 14.6\text{ mM}^{-1}$ (P-L Biochemicals). $K_{\text{m(app)}}$ and V were calculated using the program *Enzyme Kinetics* (Stanislawski, 1991). Oxaloacetate, acetoacetate and malic acid were tested for their ability to substitute for succinate as a substrate for *T. aquaticus* SCS using 20 mM of each and 3.4 µg enzyme.

2.2. Quaternary structure and stability

The stability of SCS was investigated by measuring the activity of *T. aquaticus*, *E. coli* and pig GTP-specific SCS at different temperatures and different concentrations of denaturants. For the temperature profile, enzymatic activity was measured in solutions similar to those listed above except that 10 mM potassium phosphate pH 7.4 was used as the buffer because of the small variation of its pK_{a} with temperature. 3.8 µg *T. aquaticus* SCS, 0.87 µg *E. coli* SCS and 0.82 µg pig GTP-specific SCS were used in each assay. The stability of SCS was also investigated by measuring the activity of each enzyme after incubation in 60 mM potassium phosphate pH 7.4 with different concentrations of urea (0–10 M) or guanidinium chloride (GdmCl; 0–4.0 M) for 24 h at 295 K.

Gel-filtration chromatography was performed to study the quaternary structure of *T. aquaticus* SCS in the presence and absence of GdmCl, as well as to separate the subunits. A Varian Vista 5500 liquid chromatograph was used with a Superose 12 HR 10/30 FPLC column. The flow rate was 0.5 ml min⁻¹ and, where needed, one fraction was collected each minute. Firstly, to study the quaternary structure of *T. aquaticus* SCS with no denaturants, a mixture of 5 mg ml⁻¹ each of *T. aquaticus* SCS and pig GTP-specific SCS in 5 mM β -mercaptoethanol (β -ME), 0.1 mM EDTA, 60 mM potassium phosphate pH 7.4 was separated by gel-filtration chromatography. Next, to study the quaternary structure just after *T. aquaticus* SCS had lost activity in GdmCl, 5 mg ml⁻¹ *T. aquaticus* SCS was incubated for 24 h in 1.8 M GdmCl, 5 mM β -ME, 0.1 mM EDTA, 60 mM potassium phosphate pH 7.4 and chromatography was then performed in the same buffer. Finally, *T. aquaticus* SCS was incubated in 3.0 M GdmCl, 5 mM β -ME, 0.1 mM EDTA, 60 mM potassium phosphate pH 7.4 and chromatography was performed in the same buffer.

The stability of the secondary structure of *T. aquaticus* SCS in different concentrations of GdmCl was investigated using far-ultraviolet circular dichroism (far-UV CD). The solution for far-UV CD consisted of between 0 and 7.5 M GdmCl in 5 mM β -ME, 0.1 mM EDTA, 60 mM potassium phosphate pH 7.4. The subunits were separated in 3.0 M GdmCl and then dialyzed in 5 mM β -ME, 0.1 mM EDTA, 60 mM potassium

phosphate pH 7.4; far-UV CD was performed at different concentrations of GdmCl. The concentration of whole enzyme was 9.0 or 2.2 μM , the concentration of the α -subunit was 16.2 μM and the concentration of the β -subunit was 10.0 μM . Far-UV CD measurements were made at 298 K using a Jasco J-720 spectropolarimeter (Jasco Inc., Easton, Maryland, USA) and a cuvette with a 0.02 cm path length. The instrument was routinely calibrated with ammonium D-(+)-10-camphor sulfonate at 290.5 and 192 nm and with D-(−)-pantoyllactone at 219 nm. Each sample was scanned ten times from 180 to 255 nm, measuring data every 0.05 nm. Prior to calculating molar ellipticities, noise reduction was applied to the averaged data to remove the high-frequency noise. Molar ellipticities were calculated in $\text{deg cm}^2 \text{dmol}^{-1}$ using the equation $[\theta] = \theta_{\text{obs}} \times \text{MRW}/(10 \times l \times c)$, where θ_{obs} is the ellipticity measured in millidegrees, MRW is the mean residue weight (molecular weight divided by the number of residues), l is the optical pathlength in cm and c is the protein concentration in mg ml^{-1} . Best-fit lines were fitted to the transitions using the formula $y = a + b[1 + \exp(c - x)/d]$ and the program *SigmaPlot* (Norby *et al.*, 1983).

Sedimentation-equilibrium experiments were performed to study the quaternary structure of *T. aquaticus* SCS. The analysis was first performed without GdmCl using three separate loading concentrations of *T. aquaticus* SCS: 1.77, 1.3 and 0.8 mg ml^{-1} in 2 mM DTT, 20 mM potassium phosphate pH 7.4. For analysis in the presence of GdmCl, the first GdmCl concentration used was 0.9 M, which is slightly less than that needed to inactivate the enzyme, and the second was 1.8 M GdmCl, both with 5 mM β -ME, 0.1 mM EDTA, 60 mM potassium phosphate pH 7.4. The loading concentrations of *T. aquaticus* SCS used with GdmCl were 5, 3 and 1 mg ml^{-1} . All sedimentation-equilibrium experiments were carried out at 293 K using a Beckman XL-I ultracentrifuge and interference optics according to procedures outlined by the manufacturer. Sample aliquots of 110 μl were loaded into six-sector charcoal-filled Epon sample cells, allowing the three different concentrations of protein to be run simultaneously. Runs at two different speeds were continued until there was no difference in scans that were taken 3 h apart. The sedimentation-equilibrium data were analyzed using a nonlinear least-squares curve-fitting algorithm (Johnson *et al.*, 1981) in the *NONLIN* program (D. A. Yphantis). The equation used to analyze the data assumes a single ideal species, $C_r = c[\ln(C_{r_0}) + (1 - \nu\rho)\omega/(2RT)M(r^2 - r_0^2) - BM(C_r - C_{r_0})]$, where C_r is the concentration at radius r , C_{r_0} is the concentration at the reference radius r_0 , ν is the partial specific volume, ρ is the density of the solvent, ω is the angular velocity, R is the universal gas constant, T is the temperature in kelvin, M is the molecular weight and B is the second virial coefficient associated with non-ideality. The program *SEDNTERP* (Laue *et al.*, 1992) was used to calculate the partial specific volume of the *T. aquaticus* SCS using the method of Cohn & Edsall (1943). For the runs containing GdmCl, the method of Laue was used to apply a correction to ν for the binding of GdmCl to the enzyme and the change in hydration (Laue *et al.*, 1992).

2.3. Refolding

Refolding studies were conducted by denaturing the enzyme in 6 M GdmCl for 24 h and refolding by rapid dilution [1:20(v:v)] into one of three solutions: benign buffer (50 mM KCl, 60 mM potassium phosphate pH 7.4), arginine buffer at pH 7.4 (0.67 M L-arginine-HCl, 60 mM potassium phosphate pH 7.4) or arginine buffer at pH 8.0 (0.67 M L-arginine-HCl, 60 mM potassium phosphate, 50 mM Tris-HCl pH 8.0). Samples were taken after 5 h and assayed for their ability to catalyze the formation of succinyl-CoA at pH 8.0 and 295 K. The assay solution consisted of 10 mM MgCl_2 , 50 mM KCl, 0.1 mM DTT, 10 mM succinate, 0.1 mM CoA, 0.4 mM ATP, 50 mM Tris-HCl pH 8.0. The temperature stability of the refolded enzyme was investigated by heating to 348 K for 1 h or 359 K for 20 min and then measuring the activity at pH 8.0 and 295 K. For the enzyme refolded in arginine buffer at pH 7.4, a temperature profile of the enzymatic activity was measured as had been performed for the native *T. aquaticus* SCS. Enzyme refolded in arginine buffer at pH 7.4 was exchanged into benign buffer using a Millipore centrifugal filter device and its temperature stability was tested by heating to 348 K for 1 h or 359 K for 20 min and then measuring the activity at pH 8.0 and 295 K.

To study the kinetics of refolding and its dependence on temperature, the refolding in arginine buffer at pH 7.4 was performed at 285, 295 and 310 K, taking samples at various times and measuring SCS activity at 295 K and pH 8.0. The data for the refolding were fitted to first-order kinetics and the rate constants were obtained using the program *KaleidaGraph* (Synergy Software; <http://www.synergy.com>) and replotted using an Arrhenius plot. The concentration dependence of the kinetics of refolding at 295 K was investigated by the same procedure using final protein concentrations of 0.59, 0.24 and 0.059 mg ml^{-1} in the refolding buffers.

2.4. Crystal structure of *T. aquaticus* SCS in complex with GDP-Mn²⁺

The experiments undertaken to crystallize *T. aquaticus* SCS have been described in detail by Joyce *et al.* (2007). To crystallize the full-length enzyme in complex with GDP-Mn²⁺, the protein solution consisted of 7 mg ml^{-1} protein, 5 mM GDP and 10 mM MnCl_2 . This solution was mixed with an equal volume of a precipitant solution consisting of 10% polyethylene glycol 3350 (PEG 3350), 100 mM MES pH 6.4 and 200 mM KCl and the droplet was suspended over a reservoir containing the same precipitant solution. Once a crystal grew it was transferred into similar solutions containing an incrementally increasing concentration of PEG 3350 to a maximum of 20% and was then transferred into a solution that also contained 10% glycerol before being vitrified in a stream of cold nitrogen. Crystallographic data were collected on beamline 8.3.1 of the Advanced Light Source, Berkeley, California, USA. The data were processed using the *HKL* program package (Otwinowski & Minor, 1997). Subsequent programs used to analyze the data were from the *CCP4* package (Winn *et al.*, 2011).

The structure was solved by molecular replacement using the program *AMoRe* (Navaza, 1994). The initial search models were the structures of *E. coli* SCS (Fraser *et al.*, 2002; PDB entry 1jkj) and of the α -subunit of *T. thermophilus* SCS (PDB entry 1oi7; H. Takahashi, Y. Tokunaga, C. Kuroishi, N. Babayeba, S. Kuramitsu, S. Yokoyama, M. Miyano & T. H. Tahirov, unpublished work). The models were refined using the maximum-likelihood target in the programs *CNS* (Brünger *et al.*, 1998) and *Phenix* (Adams *et al.*, 2010) with noncrystallographic symmetry restraints. The models were visualized and fitted to the electron density using the programs *Xfit* (McRee, 1999) and *Coot* (Emsley *et al.*, 2010). Stereochemistry was checked using the programs *PROCHECK* (Laskowski *et al.*, 1993), *WHATCHECK* (Hooft *et al.*, 1996) and *MolProbity* (Chen *et al.*, 2010). The programs *SPDBV* (Guex & Peitsch, 1997) and *O* (Jones *et al.*, 1991) were used to superimpose and visualize the models. The crystallographic data and the model have been deposited in the Protein Data Bank (Berman *et al.*, 2000) and were assigned the identification code 3ufx.

3. Results and discussion

3.1. Enzymatic activity

The ability of *T. aquaticus* SCS to catalyze the formation of succinyl-CoA from ATP, CoA and succinate was measured at different pH values and different temperatures. The pH profile shown in Fig. 1(a) is essentially symmetric, with maximal activity occurring between pH 8.0 and 8.4. This contrasts with the maximal activity at pH 7.4 for *E. coli* SCS (Wolodko *et al.*, 1994). The temperature profiles of these two enzymes and pig GTP-specific SCS relative to their activity at 295 K are shown in Fig. 1(b). Pig GTP-specific SCS ceased to function at 321 K, which is slightly lower than the temperature at which *E. coli* SCS became inactive (328 K). Both enzymes precipitated in

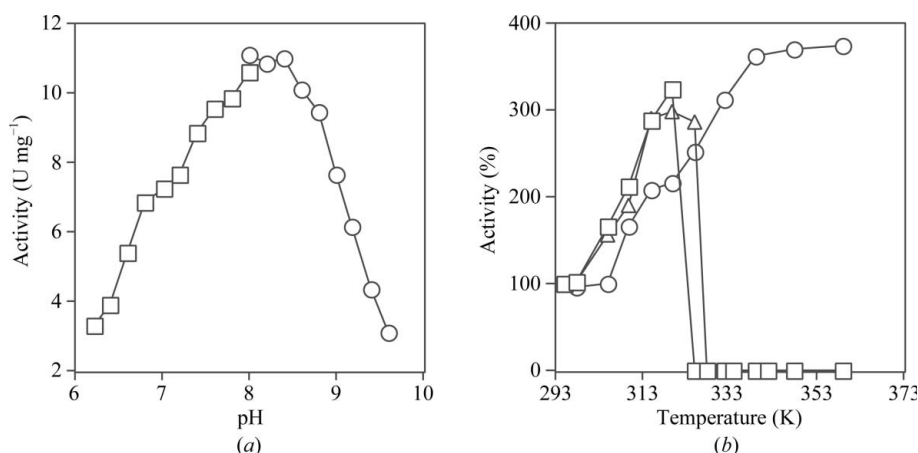


Figure 1

Enzymatic activity. (a) The activity of *T. aquaticus* SCS was measured in 10 mM MgCl₂, 50 mM KCl, 0.1 mM dithiothreitol, 10 mM succinate, 0.1 mM CoA, 0.4 mM ATP and 50 mM of either MOPS (squares) or Tris-HCl (circles) to cover the pH range 6.2–9.6. (b) The activities of *T. aquaticus* (circles), *E. coli* (triangles) and pig GTP-specific SCS (squares) in 10 mM MgCl₂, 50 mM KCl, 0.1 mM dithiothreitol, 10 mM succinate, 0.1 mM CoA, 0.4 mM ATP (for *T. aquaticus* and *E. coli* SCS) or GTP (for pig GTP-specific SCS) and 10 mM potassium phosphate pH 7.4 at different temperatures were plotted relative to their activity at 295 K.

Table 1

Kinetic parameters for *T. aquaticus* SCS at 295 K in 10 mM MgCl₂, 50 mM KCl, 50 mM Tris-HCl pH 8.0.

	ATP	GTP	CoA	Succinate
$K_{m(app)}$ (μ M)	121 \pm 5	24 \pm 5	5.5 \pm 1.0	(1.4 \pm 0.1) $\times 10^3$
V (U mg ⁻¹)	8.8 \pm 0.2	5.9 \pm 0.5	5.7 \pm 0.5	5.0 \pm 0.5

the stock solutions at the temperatures at which they became inactive. In contrast, *T. aquaticus* SCS remained soluble and active at all temperatures at which the assay could be performed. Its activity reached a plateau at approximately 339 K, with rates comparable with the values observed for *E. coli* (Wolodko & Bridger, 1987) and pig GTP-specific SCS (Fraser *et al.*, 2006) and consistent with the optimal growth temperature of 343–353 K reported for *T. aquaticus* (Brock & Freeze, 1969). Although this suggests that the reaction has reached its maximal velocity, the spontaneous hydrolysis of succinyl-CoA becomes significant at these temperatures and this could lead to anomalously low values for the enzymatic activity. The rate of hydrolysis of succinyl-CoA at 348 K was not dependent on its own concentration at 40 μ M (data not shown) and if the rate of hydrolysis of succinyl-CoA is not at all dependent on concentration, the maximum rate of synthesis of succinyl-CoA by *T. aquaticus* SCS in the presence of phosphate is 28.8 U mg⁻¹. This is also an underestimation of the true maximal rate because the phosphate buffer would reduce the specific activity measured for the enzyme, both because its pH did not match the optimal pH of the enzyme and because of product inhibition (Cha & Parks, 1964). The magnitude of the inhibition can be estimated by comparing the activity of *T. aquaticus* SCS in 10 mM potassium phosphate with that in 50 mM MOPS. At pH 7.4 and 295 K the activity in phosphate buffer is 87% of that in MOPS.

The kinetic parameters of *T. aquaticus* SCS are presented in

Table 1. $K_{m(app)}$ values for all substrates except GTP are within an order of magnitude of those determined for *E. coli* SCS (Joyce *et al.*, 1999). Surprisingly, the value of $K_{m(app)}$ for GTP is approximately 16 times less than the comparable value with *E. coli* SCS. *T. aquaticus* SCS could not use oxaloacetate, acetoacetate or malic acid to replace succinate, which is consistent with the results using *E. coli* SCS (Gibson *et al.*, 1967). As might be expected for a thermophilic enzyme operating well below its optimal temperature, the limiting rate of succinyl-CoA production at room temperature is considerably lower than the values measured for *E. coli* SCS and pig GTP-specific SCS at room temperature. The specific activities typical for *E. coli* SCS and pig GTP-specific SCS are 45 and 30 U mg⁻¹, respectively (Wolodko *et al.*, 1986).

3.2. Quaternary structure and stability

The quaternary structure of *T. aquaticus* SCS was evaluated by both gel-filtration chromatography and sedimentation equilibrium. The elution profile of a mixture of purified *T. aquaticus* and pig GTP-specific SCS revealed two separate peaks (Fig. 2a). The first was *T. aquaticus* SCS and the second was pig GTP-specific SCS, as shown by determining the activities of the protein in each peak with ATP and GTP. This elution profile resembles the elution profile of a mixture of tetrameric *E. coli* SCS and a dimeric mutant (Bailey *et al.*, 1999). The results match those of Weitzman and Kinghorn, who used SCS purified from *T. aquaticus* rather than enzyme overexpressed in *E. coli* (Weitzman & Kinghorn, 1983), and indicate that *T. aquaticus* SCS is a tetramer, since the differences in molecular weight between the subunits of *E. coli*, *T. aquaticus* and pig GTP-specific SCS are small on the scale examined by gel filtration. The interpretation is supported by sedimentation equilibrium under native conditions (Fig. 2b). These data fitted a model in which *T. aquaticus* SCS exists as a non-dissociating species with a molecular weight of 1.35×10^5 . As calculated from the amino-acid sequence deduced for our

expression plasmid (Joyce *et al.*, 2007), the weight of tetrameric *T. aquaticus* SCS would be 147 333. The conclusion is that *T. aquaticus* SCS is a heterotetramer of two α -subunits and two β -subunits.

To compare the susceptibilities of *T. aquaticus*, *E. coli* and pig GTP-specific SCS to chemical denaturation, the activity of each enzyme was measured after incubation for 24 h in various concentrations of either urea or GdmCl (Fig. 3). Pig GTP-specific SCS was the most sensitive to denaturants, *T. aquaticus* SCS was the most resistant and *E. coli* SCS was intermediate. *T. aquaticus* SCS lost activity between 4 and 5.5 M urea, but remarkably it regained activity with increasing concentrations of urea, reaching 70% of its original activity in 8.5 M urea. This behavior may have arisen from aggregation at the intermediate concentrations of urea, although no precipitation was observed. Lactate dehydrogenase from the thermophile *Thermotoga maritima* has also been shown to aggregate at intermediate concentrations of GdmCl (Dams *et*

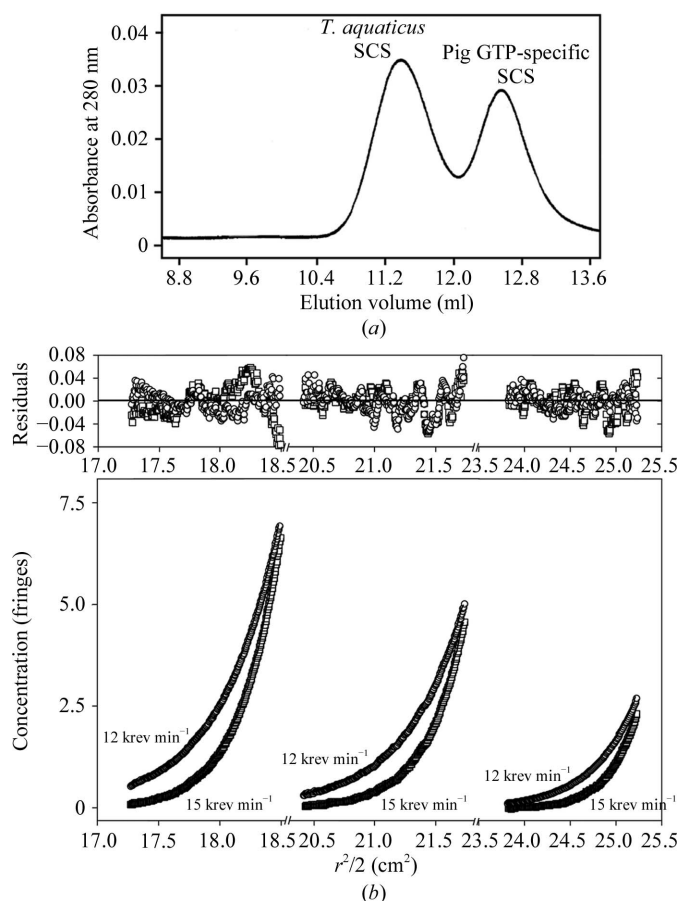


Figure 2

Quaternary structure. (a) Elution profile of *T. aquaticus* and pig GTP-specific SCS (5 mg ml⁻¹ each) from gel-filtration chromatography in 5 mM 2-mercaptoethanol, 0.1 mM EDTA, 60 mM potassium phosphate pH 7.4. (b) Sedimentation equilibrium of *T. aquaticus* SCS under native conditions using 1.77, 1.31 and 0.8 mg ml⁻¹ in 2 mM dithiothreitol, 20 mM potassium phosphate pH 7.4.

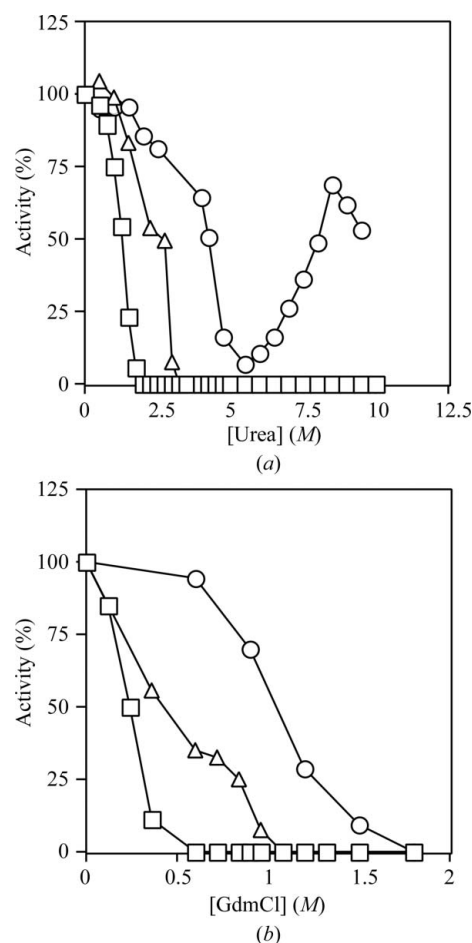


Figure 3

Chemical denaturation. The activities of *T. aquaticus* (circles), *E. coli* (triangles) and pig GTP-specific SCS (squares) were plotted relative to their activity in the absence of denaturant. The conditions for activity measurements were 10 mM MgCl₂, 50 mM KCl, 0.1 mM dithiothreitol, 10 mM succinate, 0.1 mM CoA, 0.4 mM ATP (for *T. aquaticus* and *E. coli* SCS) or GTP (for pig GTP-specific SCS), 10 mM potassium phosphate pH 7.4. (a) After 24 h incubation in 60 mM potassium phosphate pH 7.4 with urea. (b) After 24 h incubation in 60 mM potassium phosphate pH 7.4 with guanidinium chloride (GdmCl).

al., 1996). When the equilibrium unfolding of *E. coli* SCS in GdmCl was studied (Khan & Nishimura, 1988), enzymatic activity was lost prior to denaturation of the protein as monitored by far-UV CD. In addition, there were two transitions in the denaturation of *E. coli* SCS by GdmCl, with a marked plateau between them. To determine whether the equilibrium unfolding of the thermophilic enzyme from *T. aquaticus* followed the same pattern, the changes in ellipticity at 220 and 222 nm were measured as a function of the denaturant concentration using either 2.2 or 9.0 μM enzyme (Fig. 4). Unfolding was reversible at all GdmCl concentrations and was independent of the enzyme concentration. This is consistent with a very small dissociation constant for the dissociation of the whole enzyme into subunits. Reminiscent of the observations with the *E. coli* enzyme (Khan & Nishimura, 1988), there were two transitions in the denaturation curve, occurring at concentrations of 2.2 and 3.7 M GdmCl. As would be expected for a more stable enzyme, the transitions occurred at higher GdmCl concentrations than those observed for the *E. coli* enzyme (Khan & Nishimura, 1988). Similar to the results with the *E. coli* enzyme, the activity of *T. aquaticus* SCS was lost prior to the loss of secondary structure. The *T. aquaticus* enzyme had lost all SCS activity in 1.8 M GdmCl, while the changes in the molar ellipticity did not even begin until 2.0 M, indicating the presence of multiple intermediates in the unfolding process.

To investigate the nature of the intermediate that exists between the two transitions in the denaturation with GdmCl, gel-filtration chromatography of *T. aquaticus* SCS was performed in 3 M GdmCl. Two peaks were observed in the elution profile (data not shown) and the proteins in these peaks were analyzed by SDS-PAGE. The first peak consisted primarily of β -subunit and the second consisted of α -subunit alone. This raised the possibility that the first transition observed in the denaturation studies corresponded to the

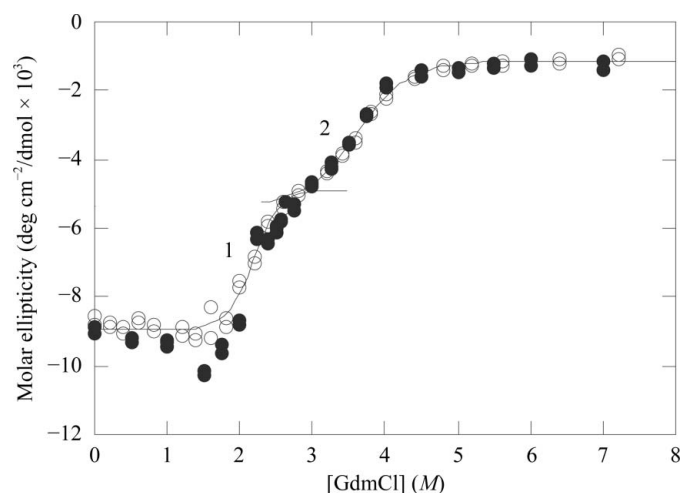


Figure 4
Equilibrium unfolding of *T. aquaticus* SCS. The changes in ellipticity were measured as a function of the concentration of denaturant using either 2.2 μM (circles) or 9.0 μM (filled circles) enzyme in 5 mM 2-mercaptoethanol, 0.1 mM EDTA, 60 mM potassium phosphate pH 7.4. The two transitions are labelled 1 and 2.

Table 2

Thermodynamic parameters for the unfolding of *T. aquaticus* SCS.

Protein	$(\Delta G_{\text{u}}^{\text{H}_2\text{O}})_{\text{app}}^\dagger$ (kJ mol ⁻¹)	m^\ddagger (kJ mol ⁻¹ M ⁻¹)	Correlation coefficient [‡]	[GdmCl] _{1/2} [‡] (M)
Whole enzyme				
First transition	29 ± 4	13 ± 2	0.986	2.2
Second transition	25 ± 1	7.1 ± 0.4	0.998	3.7
α -Subunit	6.7 ± 0.4	3.1 ± 0.2	0.998	2.2
β -Subunit	10.0 ± 0.8	5.4 ± 0.4	0.997	2.0

[†] These values were calculated by extrapolation of a replot of the molar ellipticities using the equation $\Delta G = -RT \ln K$, where $K = (\Theta_{\text{N}} - \Theta_{\text{obs}})/(\Theta_{\text{obs}} - \Theta_{\text{U}})$, Θ_{N} is the molar ellipticity observed at 0 M GdmCl, Θ_{U} is the molar ellipticity observed at the maximum concentration of GdmCl and Θ_{obs} is the observed molar ellipticity. In the vicinity of the transition the resulting plot was fitted to the equation $\Delta G = \Delta G_{\text{u}}^{\text{H}_2\text{O}} - m[\text{GdmCl}]$ (for a review, see Myers *et al.*, 1995) with the correlation coefficient listed. [‡] These values were obtained by interpolation from the graphs and are consistent with the values obtained by the calculation $[\text{GdmCl}]_{1/2} = [(\Delta G_{\text{u}}^{\text{H}_2\text{O}})_{\text{app}}/m]$.

dissociation/unfolding of the α -subunit from the tetramer of *T. aquaticus* SCS and the second transition reflected the unfolding of the remaining enzyme. To determine whether each subunit retained its native structure in the absence of the other subunit, the α -subunits and β -subunits were separated and far-UV CD was carried out on individual subunits in benign buffer. Summation of the two spectra for the individual subunits resulted in a spectrum that closely resembled the spectrum of the native enzyme in the same buffer (data not shown). This indicated that the subunits can adopt a native fold independently and thus major conformational changes are not required to form the whole enzyme from the subunits. To investigate the possibility that the denaturation of the whole enzyme was simply a sum of the denaturation of the subunits, the denaturation of each of the subunits in GdmCl was monitored by far-UV CD. The changes in molar ellipticity at 222 nm were measured as a function of the denaturant concentration. The unfolding transitions for both α -subunits and β -subunits were cooperative and reversible at all denaturant concentrations (data not shown). When the denaturation curves for the two separate subunits were added together, they did not resemble the denaturation curve for the whole enzyme, showing that the denaturation of the whole enzyme is not simply a sum of the denaturation of the individual subunits. In addition, values of $(\Delta G_{\text{u}}^{\text{H}_2\text{O}})_{\text{app}}$ and m for the transitions of the individual subunits and of the whole enzyme were calculated from replots using the molar ellipticity data (Table 2). $(\Delta G_{\text{u}}^{\text{H}_2\text{O}})_{\text{app}}$ is the free energy of unfolding, which represents the stability of the protein in water, and m is proportional to the amount of surface area that is exposed upon denaturation. All of the thermodynamic parameters associated with the transitions for the individual subunits were lower than those for the whole enzyme, indicating that the native enzyme is more stable than the isolated subunits. Thus, the denaturation of the whole enzyme is not simply a sum of the denaturation of the individual subunits, even though the subunits retain most of their native conformation when isolated. It should be noted that for the whole enzyme the calculation of $(\Delta G_{\text{u}}^{\text{H}_2\text{O}})_{\text{app}}$ assumed a two-state transition for a monomer, which was obviously not correct. However, the proper calculation for a heterotetramer requires knowledge of

the various association constants and was thus not possible. In addition, the prevalent species just prior to the beginning of the first transition in the denaturation of *T. aquaticus* SCS was observed to be a high-molecular-weight oligomer of uncertain composition with unknown association constants (data not shown).

3.3. Refolding

Since the *T. aquaticus* enzyme has the same oligomeric structure as the *E. coli* enzyme, the question of whether the refolding of *T. aquaticus* SCS follows the same path as *E. coli* SCS arises. *T. aquaticus* SCS did not refold under the conditions used for refolding either *E. coli* (Wolodko & Bridger, 1987) or pig GTP-specific SCS (Nishimura *et al.*, 1988). In the benign buffer, *T. aquaticus* SCS precipitated and less than 50% of the original activity was recovered. In addition, when refolded *T. aquaticus* SCS was heated to 348 K for 1 h or to 359 K for 20 min, enzymatic activity was lost. Refolding of *T. aquaticus* SCS appeared to be successful when carried out by rapid dilution into 0.67 M arginine, 60 mM potassium phosphate pH 7.4 or pH 8.0. No precipitate was visible and 100% of the original activity was recovered, but again this activity was not stable on heating. The thermostability of *T. aquaticus* SCS was restored by exchanging the arginine buffer for the benign buffer 50 mM KCl, 60 mM potassium phosphate pH 7.4, suggesting that the refolding was not complete in the arginine buffer.

The refolding of *T. aquaticus* SCS in arginine buffer pH 7.4 was temperature dependent and the rate of refolding followed apparent first-order kinetics. Omission of phosphate from the buffer did not affect the rate. From the Arrhenius plot, the energy of activation (E_a) associated with the refolding of *T. aquaticus* SCS was estimated to be 64.7 kJ mol⁻¹. Consistent with the results of the equilibrium unfolding of

T. aquaticus SCS, the kinetics of refolding were also not dependent on the concentration of protein tested.

Despite the high recovery of activity after refolding, the initial experiments indicated that refolded *T. aquaticus* SCS was not thermostable. To assess the stability of enzyme refolded in arginine buffer pH 7.4, its ability to catalyze the formation of succinyl-CoA was measured at different temperatures. The 'refolded' form is much less thermostable than the native form of *T. aquaticus* SCS (Fig. 5) and is only slightly more stable than the *E. coli* enzyme (compare Figs. 1a and 5). Nevertheless, refolded *T. aquaticus* SCS appeared to have full activity at 295 K when assayed in the standard manner under saturating conditions of substrates. The kinetic parameters of refolded *T. aquaticus* SCS were evaluated by steady-state analysis of initial rates of succinyl-CoA formation at 295 K, since differences in the apparent kinetic parameters compared with the native enzyme could indicate an area of the enzyme that is perturbed in the refolded enzyme. The apparent kinetic parameters were essentially the same as those of the native enzyme. Remarkably, the instability of refolded *T. aquaticus* SCS did not disturb substrate binding or catalysis at 295 K.

Studies of the conformational stability of dimeric proteins have indicated that dimerization (from monomers) leads to a substantial increase in stability. For a mutant of *E. coli* SCS that exists as an $\alpha\beta$ dimer rather than an $\alpha_2\beta_2$ tetramer, the kinetic parameters remained the same as for the wild-type enzyme but the dimer was less soluble and less stable than the wild-type tetramer (Bailey *et al.*, 1999). To investigate the possibility that the instability of *T. aquaticus* SCS was a consequence of the formation of dimeric and not tetrameric enzyme, gel-filtration chromatography of the refolded enzyme was performed. The peak of refolded *T. aquaticus* SCS eluted essentially where native *T. aquaticus* SCS eluted from the same column and well before dimeric pig GTP-specific SCS, indicating that the refolded *T. aquaticus* SCS was tetrameric.

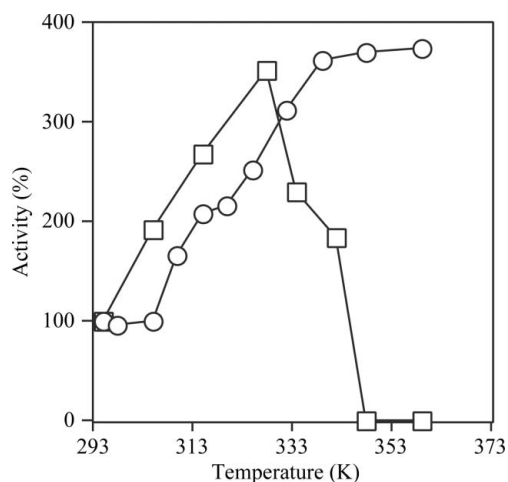


Figure 5
Thermostability. The activities of refolded *T. aquaticus* SCS (squares) and the natively folded enzyme (circles) at different temperatures are plotted. The activities were measured in 10 mM MgCl₂, 50 mM KCl, 0.1 mM dithiothreitol, 10 mM succinate, 0.1 mM CoA, 0.4 mM ATP and 10 mM potassium phosphate pH 7.4.

3.4. Crystal structure of *T. aquaticus* SCS in complex with GDP-Mn²⁺

Based on the kinetics assays, crystallization trials of *T. aquaticus* SCS included GDP in the solution with the protein. The best crystal was of *T. aquaticus* SCS in complex with GDP-Mn²⁺. Mn²⁺ can replace Mg²⁺ in catalysis, although the maximal activity of *E. coli* SCS with Mn²⁺ is lower and at a lower concentration of the ion (Gibson *et al.*, 1967). The asymmetric unit of the crystals in space group C2 includes four α -subunits (chains A, D, F and H) and four β -subunits (chains B, E, G and I). Initial electron-density maps calculated with phases from the protein showed clear electron density for GDP and the ion in each of the domains of the β -subunits possessing the ATP-grasp fold (Fig. 6). These molecules were added to the model along with water molecules possessing electron density at the 3 σ level in the difference Fourier maps and good hydrogen-bonding interactions. After refinement, the temperature factors for the nucleotides were high relative to those of the surrounding residues, suggesting that the sites

might not be fully occupied. The occupancy of each GDP-Mn²⁺ was refined and these values settled near 0.8. All residues of *T. aquaticus* SCS were fitted, except for residues 353 and 354 of chain *G*, 374–378 of chain *E* and 372–378 of chains *G* and *I* and any residues added during the cloning (Joyce *et al.*, 2007). Residues 353 and 354 of chain *G* are at a crystallographic twofold axis and the electron density suggests that they, like the residues at the carboxy-termini of the molecules, must be disordered. The protein includes one *cis*-peptide bond in each α -subunit between Gly120 α and Gly121 α and one in each β -subunit between Asn190 β and Pro191 β . Both are located at turns near catalytic residues: where the histidine that is phosphorylated during the reaction binds in the α -subunit and where Mn²⁺ binds in the β -subunit. Both of these peptide bonds are *cis* in both *E. coli* and pig GTP-specific SCS, although that in the α -subunit is between Gly and Pro. Table 3 presents the statistics for the refined model.

T. aquaticus SCS is an $\alpha_2\beta_2$ heterotetramer, but the asymmetric unit of the crystals contains an octamer, leading to confusion as to which pairs of $\alpha\beta$ dimers form the tetramers. For *E. coli* SCS, the physiologically relevant tetramer was determined by mutating residues at the dimer–dimer interface (Bailey *et al.*, 1999). By analogy to *E. coli* SCS, the *T. aquaticus* tetramers are formed by chains *A*, *B*, *D* and *E* and chains *F*, *G*, *H* and *I*.

3.4.1. Nucleotide-binding site. The crystal structure of *T. aquaticus* SCS in complex with GDP-Mn²⁺ shows how this form of SCS binds GDP. Figs. 6 and 7(a) show the interactions that lead to the binding of the guanine base. O6 and N1 of the base interact with the amide N and carbonyl O atoms of Val94 β , one of the residues forming the linker between the two subdomains adopting the ATP-grasp fold. O6 accepts a hydrogen bond from the amide N atom, while N1 donates a hydrogen bond to the carbonyl O atom. A water molecule links N7 of the base to the amine of Lys45 β and the carbonyl

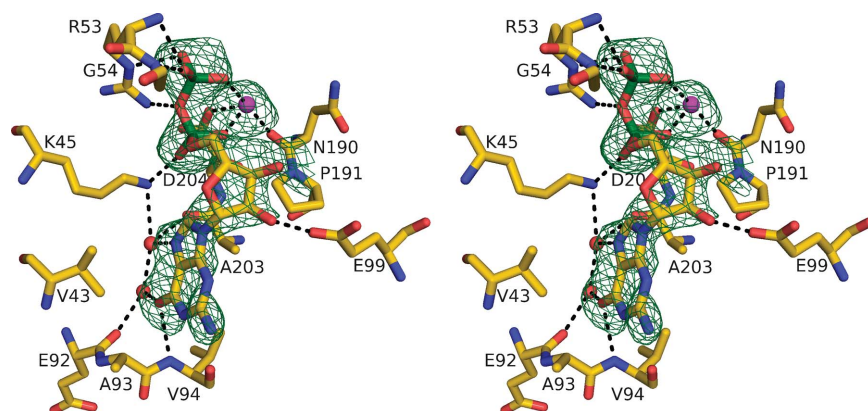


Figure 6
Complex of *T. aquaticus* SCS with GDP-Mn²⁺. In this stereoview, residues with atoms within 3.2 Å of the GDP-Mn²⁺ in chain *B* are shown, as are Glu92 β , Ala93 β , Pro191 β , Ala203 β and the water molecules that interact with the guanine base. Atoms are coloured according to type: manganese, magenta; phosphorus, green; oxygen, red; nitrogen, blue; carbon, yellow. Black dashed lines represent ionic interactions with Mn²⁺ or hydrogen bonds. The electron density, contoured at 2.5 σ and shown in green, is from an $F_o - F_c$ OMIT map calculated after refinement when GDP-Mn²⁺ had been removed from the model. This figure was drawn using the program PyMOL (DeLano, 2002).

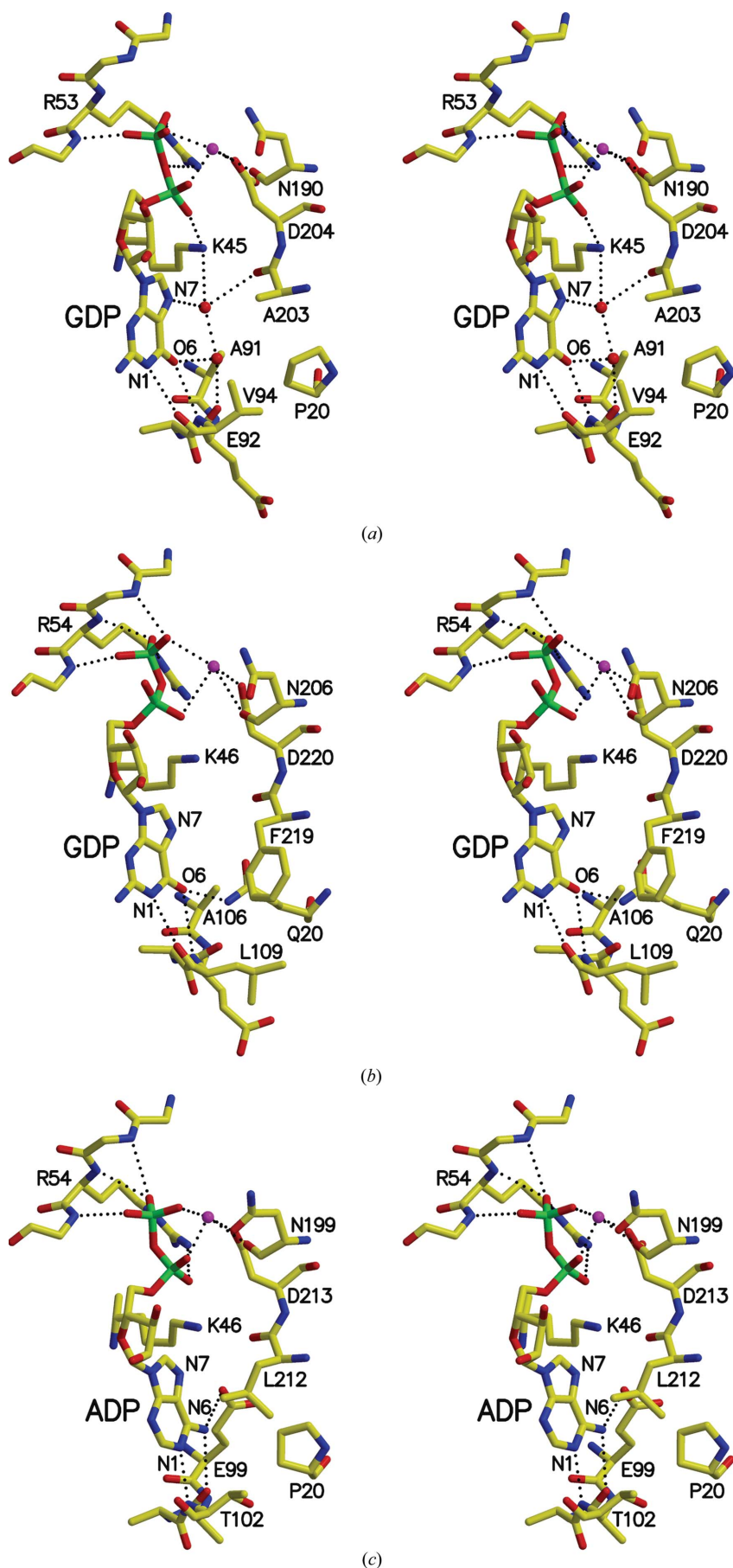
Table 3

Statistics for the refined model of *T. aquaticus* SCS in complex with GDP-Mn²⁺.

Resolution limit (Å)	2.35
Space group	C2
Unit-cell parameters (Å, °)	$a = 261.7$, $b = 126.8$, $c = 110.6$, $\alpha = \gamma = 90$, $\beta = 112.8$
R factor [†] (%) / No. of data	20.4 / 114027
$R_{\text{free}}^{\ddagger}$ (%) / No. of data	24.5 / 6048
No. of protein atoms \S	19690
No. of atoms in GDP-Mn ²⁺	116
No. of water molecules	735
R.m.s.d. for bond lengths (Å)	0.008
R.m.s.d. for bond angles (°)	1.0
Ramachandran plot, residues in	
Most favoured regions	2032 (92.4%)
Additional allowed regions	164 (7.5%)
Generously allowed regions	0
Disallowed regions	4 (0.2%)
Average temperature factors (Å ²)	
Protein atoms (range)	43 (12–139)
GDP-Mn ²⁺ atoms (range)	48 (33–65)
Water molecules (range)	36 (11–56)
Chains <i>A</i> , <i>D</i> , <i>F</i> , <i>H</i> (α -subunits)	35, 34, 36, 34
Chains <i>B</i> , <i>E</i> , <i>G</i> , <i>I</i> (β -subunits)	48, 49, 49, 49

[†] R factor = $\sum_{hkl} \sum_i |I_i(hkl) - \langle I(hkl) \rangle| / \sum_{hkl} \sum_i I_i(hkl)$. [‡] R factor based on data excluded from the refinement (~5%). \S The residues modelled are residues 1–288 of chains *A*, *D*, *F* and *H* for the α -subunit and residues 1–78 of chain *B*, 1–373 of chain *E*, 1–352 and 355–371 of chain *G* and 1–371 of chain *I* for the β -subunit.

O atom of Ala203 β (Fig. 7a) and a second water molecule links the first water molecule, O6 of the base and the carbonyl O atom of Glu92 β . This coordination of the guanine base can be compared with the binding of GDP to pig GTP-specific SCS (Fraser *et al.*, 2006; Fig. 7b) and with the binding of ADP to *E. coli* SCS (Joyce *et al.*, 2000; Fig. 7c). When GDP binds to pig GTP-specific SCS, similar interactions are formed between O6 and N1 of the base and the backbone atoms, but there is also a hydrogen-bonding interaction between NE2 of Gln20 β and O6 (Fig. 7b). N7 interacts with a water molecule bridging to Lys46 β in the complex of pig GTP-specific SCS with GTP (Fraser *et al.*, 2006). It can be presumed that a similar interaction exists in the complex with GDP (Fig. 7b), but the water molecule is not modelled in this crystal structure because of the lower resolution of the data (2.96 *versus* 2.1 Å for the complex with GTP). Gly20 β also accepts a hydrogen bond from this bridging water molecule in the complex with GTP *via* its side-chain O atom. Essentially, a water molecule and Pro20 β in *T. aquaticus* (Fig. 7a) take the place of Gln20 β in pig GTP-specific SCS (Fig. 7b), interacting well with the guanine base and residues of the nucleotide-binding site. When ADP binds to *E. coli* SCS (Fig. 7c), N6 and N1 of the adenine base interact with the backbone atoms and N6 also donates a weak hydrogen bond (3.2 Å) to Glu99 β (Joyce *et al.*, 2000). In contrast to the guanine base, N6 of the adenine base is protonated and N1 is not, so N6 donates a hydrogen bond to the carbonyl



O atom of Ala100 β of *E. coli* SCS and N1 accepts a hydrogen bond from the amide N atom of Thr102 β . Relative to GDP (Figs. 7a and 7b), the adenine base of ADP is pulled into the protein (Fig. 7c), allowing the different interactions between the atoms of the base and the backbone atoms of the residues forming the linker between the two subdomains adopting the ATP-grasp fold. In both *T. aquaticus* and pig GTP-specific SCS (Figs. 7a and 7b) there is an alanine residue in the position equivalent to Glu99 β in *E. coli* SCS (Fig. 7c). These alanine residues do not interact with the base.

T. aquaticus SCS and *E. coli* SCS will bind either ADP/ATP or GDP/GTP. For *E. coli* SCS this means that the interaction with Glu99 β (Fig. 7c) is not sufficient to give specificity for the adenine base. A similar statement can be made about *T. aquaticus* SCS: the interactions with the water molecules bridging the guanine base to Lys45 β , Ala203 β and Glu92 β (Fig. 7a) do not give specificity for the guanine base. When ADP/ATP binds to *T. aquaticus* SCS, the base would be pulled into the β -subunit as in *E. coli* SCS (Fig. 7c), so that N6 of the base could donate a hydrogen bond to the carbonyl O atom of Glu92 β and N1 could accept a hydrogen bond from the amide N atom of Val94 β . (Note that this amide N atom is the same atom that donates the hydrogen bond to O6 of the guanine base, so the change of base from guanine to adenine causes a shift along the backbone of the residues forming the linker between the two subdomains adopting the ATP-grasp fold.) A water molecule could occupy the space of the carboxylate O atom of Glu99 β of *E. coli* SCS, accepting the hydrogen bond from N6. Based on the preference of *T. aquaticus* SCS for GDP/GTP, the interactions with ADP/ATP are known to be weaker than those with GDP/GTP. However, the $K_{m(\text{app})}$ for ATP of *T. aquaticus* SCS is about the same as the $K_{m(\text{app})}$ for ATP of *E. coli* SCS (Joyce

Figure 7
Comparison of the nucleotide-binding sites of *T. aquaticus*, pig GTP-specific and *E. coli* SCS. (a) Interactions of *T. aquaticus* SCS with GDP-Mn²⁺. (b) Interactions of pig GTP-specific SCS with GDP-K⁺. (c) Interactions of *E. coli* SCS with ADP-Mg²⁺. Atoms are coloured as in Fig. 6, with the exception that either manganese, potassium or magnesium is shown in magenta. This figure and Fig. 8 were drawn using *MolScript* (Kraulis, 1991) and *Raster3D* (Merritt & Bacon, 1997).

et al., 1999). Since the residues in the nucleotide-binding site are otherwise very similar, this suggests that the change from Glu to Ala does not have a significant effect on the binding of the adenine base and that the negative charge is not important for the binding of ADP/ATP.

3.4.2. Active-site histidine residue. In all previous structures of SCS the active-site histidine residue is either phosphorylated or bound to a phosphate or a sulfate ion. As in the other structures of SCS, His246 α ND1 of *T. aquaticus* SCS forms a hydrogen bond to the side chain of Glu208 α , so it must be protonated. There is a water molecule interacting with His246 α NE2, rather than a phosphate or sulfate ion, and this water molecule bridges to a second water molecule. The second water molecule is tightly bound to residues of the two 'power helices', the helices that are donated to the active site by the α - and β -subunits (Wolodko *et al.*, 1994). This tightly bound water molecule has also been observed in the higher resolution structures of phosphorylated SCSs (Fraser *et al.*, 1999, 2000, 2006).

The residues near the catalytic histidine in *T. aquaticus* and *E. coli* SCS are similar and would not indicate a shift in the optimal pH of the enzyme. Analysis of the crystal structure of *E. coli* SCS, which has an optimal pH of 7.3–7.5, concluded that this pH was consistent with a double charge on the phosphoryl group of the phosphohistidine (Wolodko *et al.*, 1994). The catalytic mechanism would be expected to be the same for all forms of SCS, so the charge state of the phosphohistidine should be the same. Instead of the optimal pH reflecting the pK_a values for specific catalytic residues or substrates, the optimal pH could reflect optimal positioning of the residues and substrate molecules for catalysis. The diversity of optimal pH values for SCS is emphasized by the measurement of an optimal pH of 6 for yeast SCS (Schwartz *et al.*, 1983).

The only cysteine residue in *T. aquaticus* SCS is Cys123 α , which is located near the catalytic histidine and after the *cis*-peptide bond that links Gly120 α and Gly121 α . This cysteine residue is highly conserved in SCSs (Hidber *et al.*, 2007). Lower proportions of cysteine residues have been observed in thermophilic prokaryotes compared with mesophiles (Singer & Hickey, 2003) and are thought to diminish the chance of oxidation, which would occur more readily at higher temperatures. In the structure of *T. aquaticus* SCS this cysteine residue is buried; it is protected in part by the turn formed by Gly120 α -Gly121 α -Asn122 α and Pro124 α .

3.4.3. Proposed succinate-binding site. The succinate-binding site in SCSs was proposed based on the binding of citrate to ATP-citrate lyase (Sun *et al.*, 2010). The binding site is located on a loop of the β -subunit near the two power helices. The carboxylate group of succinate that does not take part in the catalytic reaction is expected

to interact with the backbone N atoms of Gly321 β and Val323 β of *E. coli* SCS or Gly328 β and Val330 β of pig GTP-specific SCS. In *T. aquaticus* SCS the equivalent residues are Gly312 β and Thr314 β . The loop that includes these residues has a different conformation in each of the three enzymes, providing no further information on the binding site (Fig. 8). The glycine residues in this loop are likely to provide the flexibility observed in the structures of the different SCSs in the absence of succinate. What is consistent in the structures is that this loop is constrained by hydrogen bonds at the two ends. At the amino-terminal end an asparagine side chain forms hydrogen bonds to the amide N atom and carbonyl O atom of Phe319 β , Phe326 β or Phe310 β in *E. coli*, pig GTP-specific or *T. aquaticus* SCS, respectively. At the carboxy-terminal end a hydrogen bond is donated by the amide N atom of residue Cys325 β , Cys332 β or Ala316 β in *E. coli*, pig GTP-specific or *T. aquaticus* SCS, respectively, to a carbonyl O atom of a residue on the neighbouring loop: Asn352 β , Thr359 β or Thr343 β in *E. coli*, pig GTP-specific or *T. aquaticus* SCS, respectively. In each case, the phenylalanine residue is the penultimate residue of the β -strand preceding the loop and the cysteine or alanine residue is followed by an α -helix (Fig. 8).

3.4.4. Stability enhancement. The crystal structure suggests some residues that are important in enhancing the thermostability of *T. aquaticus* SCS and its resistance to chemical denaturation. A simple comparison of the residue content of *T. aquaticus*, *E. coli* and pig GTP-specific SCS shows the trend that the more stable the SCS, the lower the content of cysteine, serine, phenylalanine, asparagine and glutamine residues and the higher the content of alanine, valine, methionine, histidine and arginine residues. This is generally consistent with the comparison of protein sequences from mesophilic and thermophilic *Methanococcus* species, which showed fewer uncharged polar residues and more charged residues (Haney *et al.*, 1999). Examination of the structures shows 15 salt

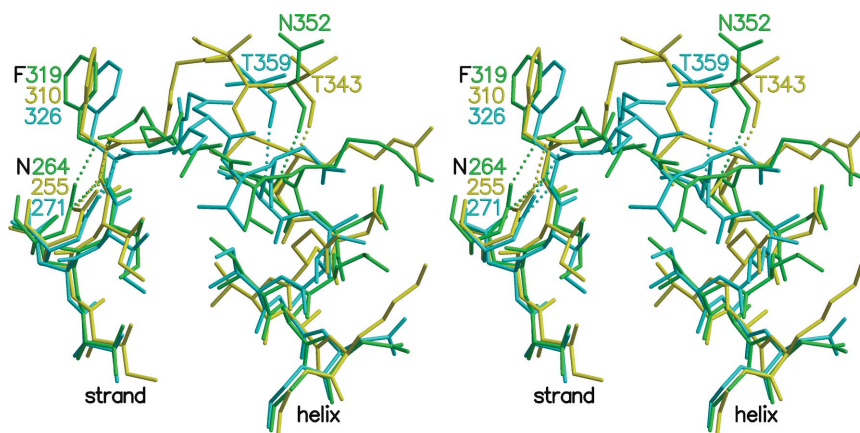


Figure 8

Comparison of the proposed succinate-binding sites of *T. aquaticus*, pig GTP-specific and *E. coli* SCS. The three structures were superposed based on the positions of the backbone atoms of the last five residues in the β -strand preceding the loop and the first six residues in the α -helix following the loop. *T. aquaticus* SCS is shown in yellow, pig GTP-specific SCS (PDB entry 2fp4; Fraser *et al.*, 2006) is shown in cyan and *E. coli* SCS (PDB entry 1cqi; Joyce *et al.*, 2000) is shown in green. Hydrogen bonds constraining the ends of the loop are shown as dashed lines.

bridges that are present in *T. aquaticus* SCS but not in either *E. coli* or pig GTP-specific SCS. Six are between arginine and glutamate residues, three between arginine and aspartate residues, four between lysine and glutamate residues and two between lysine and aspartate residues. Ionic interactions have been proposed to be a major stabilizing feature of glutamate dehydrogenase from the hyperthermophile *Pyrococcus furiosus* (Rice *et al.*, 1996).

4. Conclusions

The structure of *T. aquaticus* SCS in complex with GDP-Mn²⁺ shows how changes in specific residues within the ATP-grasp fold can shift the nucleotide preference. Like *E. coli* SCS, *T. aquaticus* SCS has a proline residue at position 20 of the β -subunit. *T. aquaticus* SCS also has an alanine residue in the β -subunit where *E. coli* SCS has a glutamate residue. The smaller alanine residue allows an additional water molecule to bind between the proline and the guanine base. This gives a preference for GDP/GTP over ADP/ATP by providing similar interactions for the guanine base as observed for the glutamine residue at position 20 of the β -subunit of pig GTP-specific SCS.

A Discovery Grant from the Natural Sciences and Engineering Research Council of Canada (NSERC) funded the characterization using X-ray crystallography. Crystallographic data were collected on beamline 8.3.1 at the Advanced Light Source (ALS) at Lawrence Berkeley Laboratory under an agreement with the Alberta Synchrotron Institute (ASI). The ALS is operated by the Department of Energy and supported by the National Institutes of Health. Beamline 8.3.1 was funded by the National Science Foundation, the University of California and Henry Wheeler. The ASI synchrotron-access program is supported by grants from the Alberta Science and Research Authority and the Alberta Heritage Foundation for Medical Research (AHFMR). The Canadian Institutes of Health Research supported the research characterizing the enzyme in solution. We thank Kim Oikawa in the laboratory of Dr Cyril Kay for conducting circular-dichroism measurements.

References

- Adams, P. D. *et al.* (2010). *Acta Cryst. D* **66**, 213–221.
- Bailey, D. L., Fraser, M. E., Bridger, W. A., James, M. N. & Wolodko, W. T. (1999). *J. Mol. Biol.* **285**, 1655–1666.
- Berman, H. M., Westbrook, J., Feng, Z., Gilliland, G., Bhat, T. N., Weissig, H., Shindyalov, I. N. & Bourne, P. E. (2000). *Nucleic Acids Res.* **28**, 235–242.
- Bridger, W. A. (1971). *Biochem. Biophys. Res. Commun.* **42**, 948–954.
- Bridger, W. A. (1974). *The Enzymes*, edited by P. D. Boyer, Vol. 10, pp. 581–606. New York: Academic Press.
- Brock, T. D. & Freeze, H. (1969). *J. Bacteriol.* **98**, 289–297.
- Brownie, E. R. & Bridger, W. A. (1972). *Can. J. Biochem.* **50**, 719–724.
- Brünger, A. T., Adams, P. D., Clore, G. M., DeLano, W. L., Gros, P., Grosse-Kunstleve, R. W., Jiang, J.-S., Kuszewski, J., Nilges, M., Pannu, N. S., Read, R. J., Rice, L. M., Simonson, T. & Warren, G. L. (1998). *Acta Cryst. D* **54**, 905–921.
- Cha, S. & Parks, R. E. (1964). *J. Biol. Chem.* **239**, 1968–1977.
- Chen, V. B., Arendall, W. B., Headd, J. J., Keedy, D. A., Immormino, R. M., Kapral, G. J., Murray, L. W., Richardson, J. S. & Richardson, D. C. (2010). *Acta Cryst. D* **66**, 12–21.
- Cohn, E. J. & Edsall, J. T. (1943). *Proteins, Amino Acids and Peptides as Ions and Dipolar Ions*. New York: Reinhold.
- Dams, T., Ostendorp, R., Ott, M., Rutkat, K. & Jaenicke, R. (1996). *Eur. J. Biochem.* **240**, 274–279.
- DeLano, W. L. (2002). *PyMOL*. <http://www.pymol.org>.
- Deng, J., Davies, D. R., Wisedchaisri, G., Wu, M., Hol, W. G. J. & Mehlin, C. (2004). *Acta Cryst. D* **60**, 203–204.
- Emsley, P., Lohkamp, B., Scott, W. G. & Cowtan, K. (2010). *Acta Cryst. D* **66**, 486–501.
- Fraser, M. E., Hayakawa, K., Hume, M. S., Ryan, D. G. & Brownie, E. R. (2006). *J. Biol. Chem.* **281**, 11058–11065.
- Fraser, M. E., James, M. N., Bridger, W. A. & Wolodko, W. T. (1999). *J. Mol. Biol.* **285**, 1633–1653.
- Fraser, M. E., James, M. N., Bridger, W. A. & Wolodko, W. T. (2000). *J. Mol. Biol.* **299**, 1325–1339.
- Fraser, M. E., Joyce, M. A., Ryan, D. G. & Wolodko, W. T. (2002). *Biochemistry*, **41**, 537–546.
- Gibson, J., Upper, C. D. & Gunsalus, I. C. (1967). *J. Biol. Chem.* **242**, 2474–2477.
- Guex, N. & Peitsch, M. C. (1997). *Electrophoresis*, **18**, 2714–2723.
- Haney, P. J., Badger, J. H., Buldak, G. L., Reich, C. I., Woese, C. R. & Olsen, G. J. (1999). *Proc. Natl Acad. Sci. USA*, **96**, 3578–3583.
- Hidber, E., Brownie, E. R., Hayakawa, K. & Fraser, M. E. (2007). *Acta Cryst. D* **63**, 876–884.
- Hooft, R. W., Vriend, G., Sander, C. & Abola, E. E. (1996). *Nature (London)*, **381**, 272.
- Johnson, M. L., Correia, J. J., Yphantis, D. A. & Halvorson, H. R. (1981). *Biophys. J.* **36**, 575–588.
- Johnson, J. D., Mehus, J. G., Tews, K., Milavetz, B. I. & Lambeth, D. O. (1998). *J. Biol. Chem.* **273**, 27580–27586.
- Johnson, J. D., Muhonen, W. W. & Lambeth, D. O. (1998). *J. Biol. Chem.* **273**, 27573–27579.
- Jones, T. A., Zou, J.-Y., Cowan, S. W. & Kjeldgaard, M. (1991). *Acta Cryst. A* **47**, 110–119.
- Joyce, M. A., Brownie, E. R., Hayakawa, K. & Fraser, M. E. (2007). *Acta Cryst. F* **63**, 399–402.
- Joyce, M. A., Fraser, M. E., Brownie, E. R., James, M. N., Bridger, W. A. & Wolodko, W. T. (1999). *Biochemistry*, **38**, 7273–7283.
- Joyce, M. A., Fraser, M. E., James, M. N., Bridger, W. A. & Wolodko, W. T. (2000). *Biochemistry*, **39**, 17–25.
- Khan, I. A. & Nishimura, J. S. (1988). *J. Biol. Chem.* **263**, 2152–2158.
- Kraulis, P. J. (1991). *J. Appl. Cryst.* **24**, 946–950.
- Laskowski, R. A., MacArthur, M. W., Moss, D. S. & Thornton, J. M. (1993). *J. Appl. Cryst.* **26**, 283–291.
- Laue, T. M., Shah, B. D., Ridgeway, T. M. & Pelletier, S. L. (1992). *Analytical Ultracentrifugation in Biochemistry and Polymer Science*, edited by S. E. Harding, A. J. Rowe & J. C. Horton, pp. 90–125. Cambridge: Royal Society of Chemistry.
- Luo, L., Pappalardi, M. B., Tummino, P. J., Copeland, R. A., Fraser, M. E., Grzyska, P. K. & Hausinger, R. P. (2006). *Anal. Biochem.* **353**, 69–74.
- McRee, D. E. (1999). *J. Struct. Biol.* **125**, 156–165.
- Merritt, E. A. & Bacon, D. J. (1997). *Methods Enzymol.* **277**, 505–524.
- Myers, J. K., Pace, C. N. & Scholtz, J. M. (1995). *Protein Sci.* **4**, 2138–2148.
- Navaza, J. (1994). *Acta Cryst. A* **50**, 157–163.
- Nishimura, J. S. (1986). *Adv. Enzymol. Relat. Areas Mol. Biol.* **58**, 141–172.
- Nishimura, J. S., Ybarra, J., Mitchell, T. & Horowitz, P. M. (1988). *Biochem. J.* **250**, 429–434.
- Norby, J., Rubenstein, S., Tuerke, T., Schwallie Farmer, C., Forood, R. & Bennington, J. (1983). *SigmaPlot: Scientific Graph System*, v4.11. SPSS Inc., Chicago, USA.
- Otwinowski, Z. & Minor, W. (1997). *Methods Enzymol.* **276**, 307–326.

- Rice, D. W., Yip, K. S., Stillman, T. J., Britton, K. L., Fuentes, A., Connerton, I., Pasquo, A., Scandura, R. & Engel, P. C. (1996). *FEMS Microbiol. Rev.* **18**, 105–117.
- Schwartz, H., Steitz, H. O. & Radler, F. (1983). *Antonie van Leeuwenhoek*, **49**, 69–78.
- Singer, G. A. & Hickey, D. A. (2003). *Gene*, **317**, 39–47.
- Stanislawski, J. (1991). *Enzyme Kinetics*, v.1.11. Trinity Software, Campton, New Hampshire, USA.
- Sun, T., Hayakawa, K., Bateman, K. S. & Fraser, M. E. (2010). *J. Biol. Chem.* **285**, 27418–27428.
- Weitzman, P. D. J. & Kinghorn, H. A. (1983). *FEBS Lett.* **154**, 369–372.
- Winn, M. D. *et al.* (2011). *Acta Cryst.* **D67**, 235–242.
- Wolodko, W. T. & Bridger, W. A. (1987). *Biochem. Cell Biol.* **65**, 452–457.
- Wolodko, W. T., Fraser, M. E., James, M. N. & Bridger, W. A. (1994). *J. Biol. Chem.* **269**, 10883–10890.
- Wolodko, W. T., Kay, C. M. & Bridger, W. A. (1986). *Biochemistry*, **25**, 5420–5425.